Available online at www.sciencedirect.com
ScienceDirect
Construction and Building Materials 23 (2009) 78–84
Construction and Building MATERIALS
www.elsevier.com/locate/conbuildmat

Effect of various dual-phase heat treatments on the corrosion behavior of reinforcing steel used in the reinforced concrete structures

Oğuzhan Keleştemur *, Servet Yıldız

Technical Education Faculty Construction Department, Firat University, Elazig 23119, Turkey

Received 3 November 2007; received in revised form 16 January 2008; accepted 1 February 2008
Available online 10 March 2008

Abstract

In this study, corrosion behavior of six different dual-phase (DP) steels with varying morphologies and martensite content has been examined in comparison to ferrite–pearlite steel in concrete. Intercritical annealing and intermediate quenching heat treatments have been applied to the reinforcing steel in order to obtain DP steels with different morphologies and content of martensite. Corrosion experiments were conducted in two stages. In the first stage, the corrosion potential of steels embedded in concrete was measured every day for a period of 30 days in accordance with ASTM C 876 standard. In the second stage, anodic and cathodic polarization values of these steels were obtained and then the corrosion currents were determined with the aid of cathodic polarization curves. It has been observed that both the amount of martensite and the morphology of the phase constituents have definite effect on the corrosion behavior of DP steel embedded in concrete. As a result of this study, it is found that corrosion rate of dual-phase steel has increased with increase amount of martensite.

Keywords: Dual-phase steel; Corrosion; Concrete; Microstructure; Martensite

1. Introduction

Corrosion of reinforcing steel in concrete has been recognized as a serious problem throughout the world [1,2]. Concrete structures, bridges, buildings, sanitary and water facilities and other reinforced concrete structures get severely damaged due to corrosion of the reinforcing steel. The resultant cracking and spalling of the concrete cost billions of dollars each year. The estimated corrosion damage of bridge deck and support structures in the USA alone ranges between $170 and $550 million. It has been estimated that replacement cost of concrete structures could be substantially higher [3]. In addition to the economic losses incurred, public safety is also affected. Loss of life associated with the collapse of bridges and structures are examples.

Use of reinforced concrete structures is based on the principle that concrete is an ideal environment for steel. The highly alkaline medium of the Portland cement causes iron to passivity. Such passivity is generally described as the formation of a minute protective layer consisting mainly of gamma Fe_2O_3 which prevents further corrosion. It is this formation of a passivating film that makes reinforced concrete such a desirable building material. However, continuous exposure to corrosive environmental conditions, added with steady deterioration with time due to thermal effects, seepage, mechanical abuses, etc., lead to corrosion and failure of concrete structure and consistent fall of residual life [4].

Several approaches can be followed to obtain durable reinforced concrete structures. One approach is to improve the quality of the plain concrete with the use of mineral admixtures to lower the permeability of the material, thus decreasing the ingress of deleterious substances and delaying depassivation of the steel [5–7]. An alternative and complementary approach is to improve the durability of

* Corresponding author. Fax: +90 424 2367064.
E-mail address: okelestemur@firat.edu.tr (O. Keleştemur).

0950-0618/$ - see front matter © 2008 Elsevier Ltd. All rights reserved.
doi:10.1016/j.conbuildmat.2008.02.001

the reinforcing steel. Epoxy coated and galvanized reinforcing steels have been marketed to alleviate the problems of corrosion of steel in concrete structures, but recent studies have shown that these treated bars only delay the initiation of corrosion [8,9].

Developed in 1970s dual-phase steels consisting of soft ferrite and hard martensite has received enormous attention over the last three decades. Dual-phase steels are a special derivative of the high strength low alloy (HSLA) steels. Large volume of literature now exists on the processing and correlations of microstructural parameters with different mechanical properties. The early investigations have revealed that DP steels possess a number of unique properties making them attractive for application as very good quality sheet materials for automotive industries. These include a continuous yielding, low 0.2% offset yield strength, high tensile strength and high uniform and total elongations [10,11]. The unique combination of mechanical properties has led the researchers to explore the suitability of DP steels for structural and constructional purposes through replacement of pearlite wire, rods and bars [12–16]. Besides very good combination of mechanical properties, a priori knowledge about the corrosion behavior of DP steels is essential for assessing the true potential of DP steels in such applications [17]. Investigations in this direction though extremely limited, Jha et al. [14], Thomas [13] and Zhang et al. [18], have observed very good corrosion resistance properties out of dual-phase microstructure. Trejo et al. [19] have also observed that DP steels has better corrosion resistance than standard billet reinforcement in concrete. But, it is possible to find different approaches in the open literature. For example, Sarkar et al. [17] were tried to enhance the martensite content to improve mechanical properties of DP steels. However results of this study showed worse corrosion behavior of DP steel in 3.5% NaCl solution. The studies performed to determine corrosion behavior of dual-phase steel has not cleared the subject enough. Therefore, further studies on corrosion behavior of dual-phase steels, especially in concrete is needed for effective use of these steels in construction industry.

In this work, dual-phase steels with different morphologies were obtained by different heat-treating a SAE1010 structural carbon steel which is cheap and wide range of use in the construction industry at different conditions. The effect of morphology on the corrosion behavior of these dual-phase steel embedded in concrete have been investigated.

2. Experimental

2.1. Material and heat treatment

As an electrode, Ereğli Iron and Steel Factories in Turkey product SAE1010 steel a bar, which is the fundamental construction material of construction industry, were selected for the present study. The as-received material was in the form of 12 mm diameter hot rolled bar with a ferritic–pearlitic structure. The chemical composition of SAE1010 is given in Table 1.

The critical temperatures of the steel were determined by microscopic examination of heat treated specimens. Starting at 680 °C the specimens were heat treated in neutral salt bath for environmental protection and then quenched in a mixture of ice + water. The procedure was repeated at 10 °C intervals. From the microscopic examinations, 730 °C and 840 °C were found to be sufficiently close to the A_1 and A_3 (critical temperatures of the iron–carbon equilibrium diagram of steel) temperature, respectively. However, at temperatures above 840 °C, it was not possible to transform the austenite to martensite effectively due to the low carbon content of austenite which impaired its hardenability. The specimens were heat treated at 730 °C to increase carbon content in austenite phase.

Small specimens of 15 mm in length were cut out from the as-received material for metallographic examinations. Corrosion specimens of 110 mm in length were also cut out from the as-received material. All specimens were subjected to different heat treatment procedures as follows:

- Hold at 730 °C ($\alpha + \gamma$ region) for 25, 50, 75 min → -quench, intercritical annealing (IA25, IA50, IA75).
- Hold at 900 °C (γ region) for 1 h → quench, then reheat 730 °C and hold for 25, 50, 75 min → quench, intermediate quenching (IQ25, IQ50, IQ75).

All the heat treatment cycles were carried out in a neutral salt bath whose temperature was controlled at ±1 °C for atmospheric environmental protection and then quenched in a mixture of ice + water.

Microstructure of the specimens were observed under light microscope following usual metallographic polishing and etching with 2% nital solution. Volume fraction of the phase constituents has been determined by the method given in ASTM E112 [20].

2.2. Corrosion tests

A total of 35 concrete blocks were prepared to investigate corrosion behavior of the dual-phase steel produced from reinforcing steel bar. Steel samples embedded in 100 × 100 × 200 mm concrete blocks were evaluated for corrosion behavior.

ASTM C 150 Type I Portland cement was used in order to prepare all concrete samples included in the experiments in scope of the study. Chemical composition of this cement is given in Table 2. The cement used in concrete mixture has 3.1 g/cm^3 specific gravity. Tap water was used as mix

Table 1
Chemical composition of the steel (wt.%)

C	Si	Mn	S	Fe
0.176	0.231	0.557	0.027	Balance

Table 2
Chemical composition of cement (wt.%)

SiO_2	Al_2O_3	Fe_2O_3	CaO	MgO	SO_3	Cl^-	LOI	Unknown
22.05	5.40	3.18	63.07	2.21	2.20	0.009	1.29	1.80

water while preparing the concrete blocks. 3.5% NaCl was added into the mix water of the concrete mortar for the sake of creating corrosive environment. The concrete mixture has a water–cement ratio of 0.55 and a wet unit weight was 2237 kg/m^3.

Mixture ratio of concrete blocks in compliance with ACI 211.1 [21] is presented in Table 3.

Corrosion experiments were conducted in two stages. In the first stage, the corrosion potential of steels embedded in concrete were measured every day for a period of 30 days in accordance with ASTM C-876 method [22]. In the second stage, anodic and cathodic polarization values of steel embedded in concrete were obtained and then the corrosion currents were determined with the aid of cathodic polarization curves.

Sixty DP steel bars were machined to 11 mm diameter and 9 cm length to remove the decarburized layer and sample surfaces were polished with 1200 mesh sandpaper. Polished surfaces were cleaned with ethyl alcohol. 10 cm^2 surface areas were left open in the tips of electrodes which will be embedded in the concrete. Screw thread was machined in other ends of steel electrodes and cables were connected to these ends in order to easily make measurements during the experiment. Remaining sections of the electrodes were protected against external effects by covering with epoxy resin at first and then with polyethylene wrap. Then the electrodes placed in 10 × 10 × 20 cm concrete blocks. Ten reinforced steel bars in the as-received normal condition (i.e., as used construction practice) were also placed in similar forms in order to carry out corrosion experiments.

Table 3
Mixture proportion of concrete blocks (kg/m^3)

Cement	Water	Gravel (4–8 mm)	Sand (0–4 mm)	NaCl
400	220	560	1043	6.6

Experimental setup used for the application of galvanostatic method is shown schematically in Fig. 1.

Black areas on the electrodes displayed in Fig. 1 indicate the areas kept under protection.

3. Results and discussion

3.1. Microstructure

Microstructure of the as-received specimen (FP) shown in Fig. 2 reveals that the structure consist of uniformly distributed pearlite colonies in an equiaxed ferrite matrix.

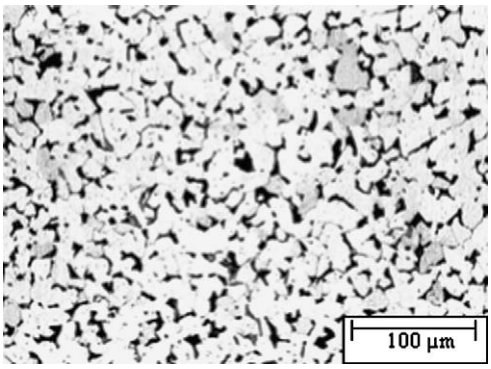

Fig. 2. Ferrite–pearlite structures being processed to produce dual-phase steel.

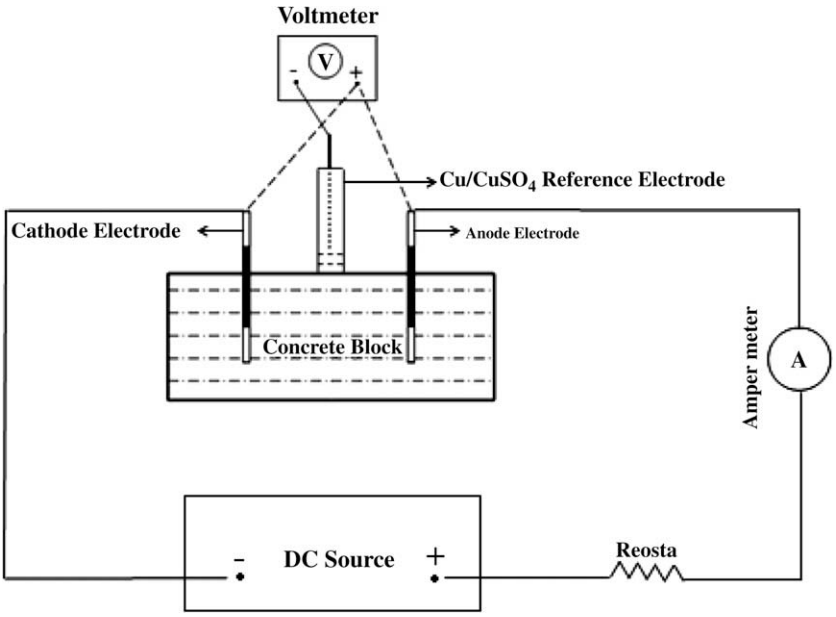

Fig. 1. Schematic representation of the polarization measurement using galvanostatic method.

Microstructures of DP steels are shown in Figs. 3 and 4. It is observed that heat-treating of FP specimen directly to the intercritical temperature results in the development of martensite network surrounding ferrite grains (Fig. 3). Such morphological distribution of martensite is commonly termed as ring, chain or continuous network of martensite [17]. Initially, microstructure of the IA specimen has ferrite and pearlite. When annealed in the ($\alpha + \gamma$) region,

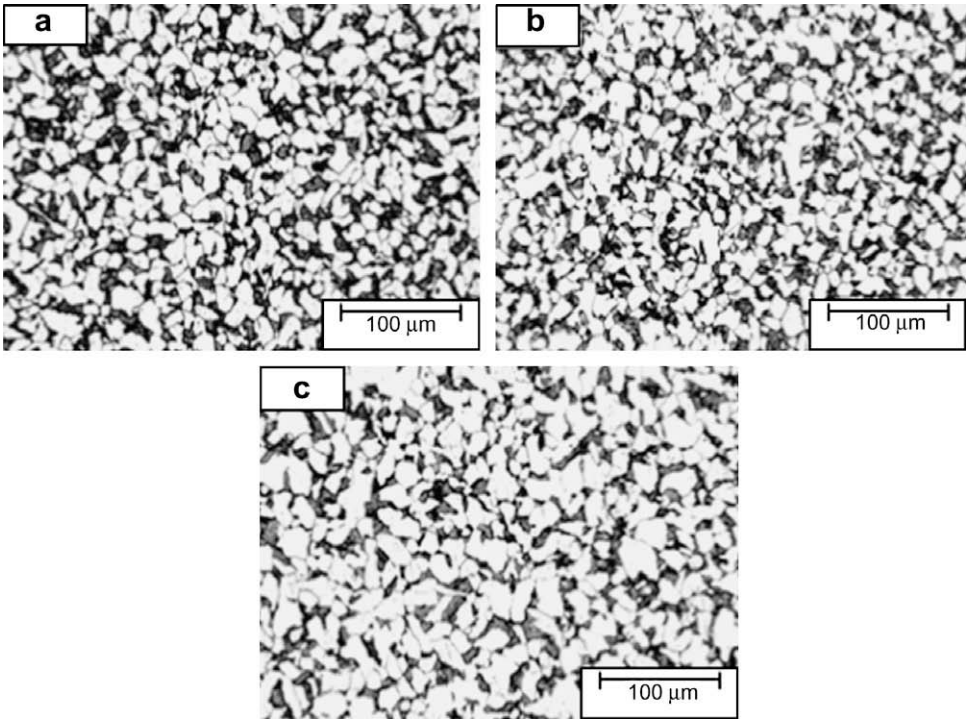

Fig. 3. Microstructures of IA specimens: (a) IA75, (b) IA50, (c) IA25.

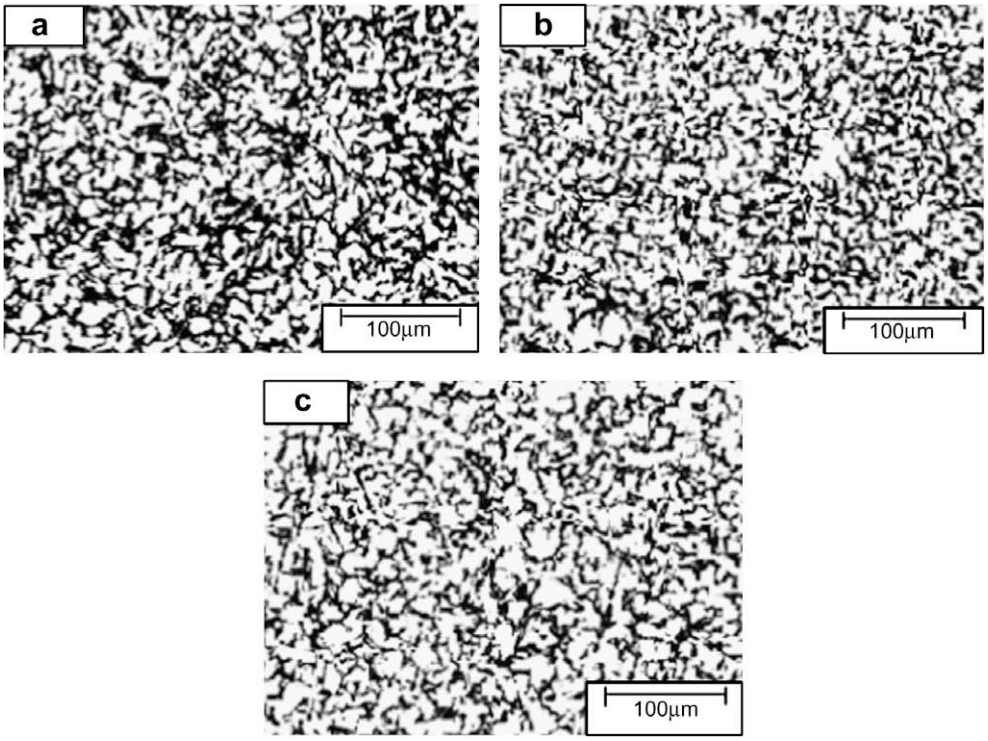

Fig. 4. Microstructures of IQ specimens: (a) IQ75, (b) IQ50, (c) IQ25.

austenite grains are nucleated at the carbide/ferrite interfaces, which transform to martensite after water quenching. On the other hand, the IQ specimen reveals a martensitic structure after water quenching, and then retransform to ferrite and martensite phases via water quenching from ($\alpha + \gamma$) region. It was noticed that the IQ specimen revealed more ragged grain boundaries and smaller ferrite grains as compared to the IA specimen. However, lath martensites were more evenly distributed in the IQ specimen as shown in Fig. 4. Such finely distributed phase mixtures consisting of ferrite and martensite are commonly termed as a fibrous structure. The observed difference in the evolution of microstructure in the IA and IQ specimens after intercritical annealing is apparently due to the differences in the microstructural state of the samples before they are subjected to the intercritical annealing. It may be noted that in case of IQ specimens the microstructures are completely martensitic prior to intercritical annealing, whereas the microstructures of IA specimens are ferrite and pearlite before intercritical annealing.

Microstructures of specimens (IA25, IQ25) developed using the lowest duration for austenization treatment brought no essential change in the morphology of phase constituents in comparison to that of IA75 or IQ75 specimens, respectively. It is thus revealed that microstructures before intercritical annealing bear a tremendous influence on the morphology and distribution of the phase constituents.

The changes on the volume fraction of the phases are shown in Table 5.

3.2. Corrosion behavior

The corrosion potential of steels embedded in concrete were daily measured for a period of 30 days in accordance with ASTM C-876 standard. Saturated copper/copper sulfate (CSE) was used as the reference electrode, and a high impedance voltmeter was used as the measurement device in corrosion potential measurements. Changes in corrosion potentials with time were indicated as graphics in order to determine whether the steel is in active or passive state.

The results obtained from corrosion potential measurements of the steels embedded in concrete samples are indicated in Figs. 5 and 6.

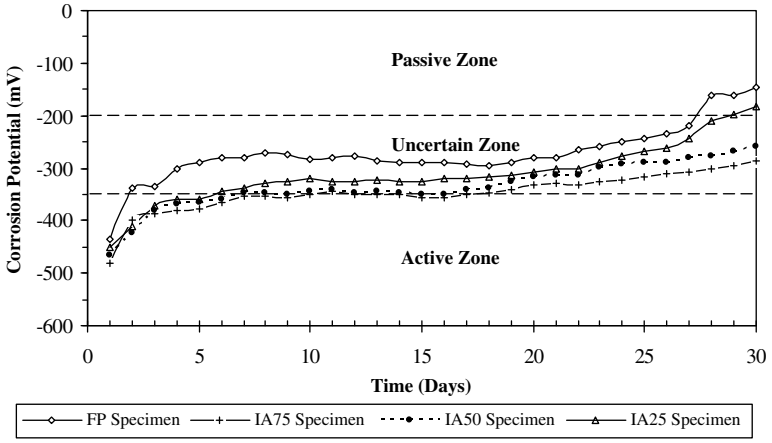

Fig. 5. The change of the corrosion potential on the FP, IA25, IA50, IA75 specimens.

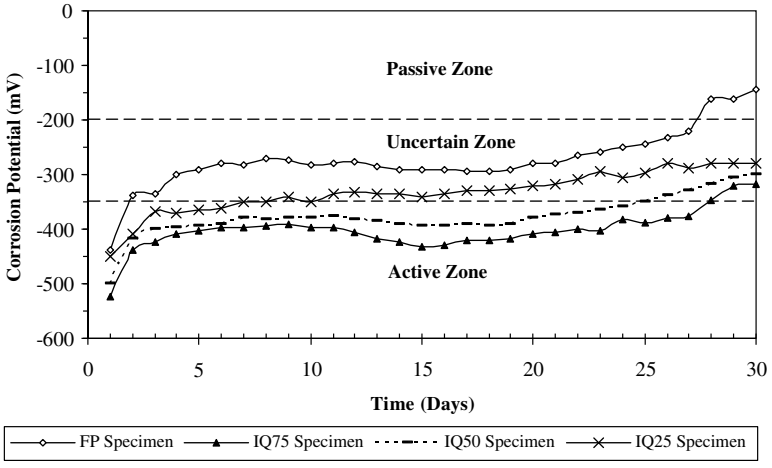

Fig. 6. The change of the corrosion potential on the FP, IQ25, IQ50, IQ75 specimens.

Recommendations on evaluation of potential measurement results in ASTM C-876 experiment method are stated in Table 4.

As seen in Figs. 5 and 6, the corrosion rate is higher in all DP steels of any type compare to FP steel, some amount of decrease appeared in corrosion rate depending on reduce in the amount of martensite. Indeed, FP specimen became more passive compare to the IQ specimens and reached to passive zone in terms of corrosion at the end of the 27th day, IQ specimens remained in the uncertain zone even at the end of 30th day. Nevertheless, IA specimens became more passive than IQ specimens. As seen Fig. 5, while IA25 specimen was in the passive zone at the end of the 27th day with together FP specimen, the all IQ specimens stayed in the uncertain zone. In addition, IQ50 and IQ75 in which martensite amount was high could pass to uncertain region not until the third week although IA specimens pass to uncertain region at the end of the 27th day. It indicates that IA dual-phase steels have higher corrosion resistance than IQ dual-phase steels. From the results of corrosion potentials by ASTM C-876 standard it can be said that corrosion behavior of DP steels inside the concrete change depending on the microstructure but the steels with a microstructure of ferrite and pearlite have a higher corrosion resistance than dual-phase steels.

The corrosion potential provides qualitative and probably indicates on corrosion of steel embedded in concrete. Quantitative and reliable information on corrosion of steel embedded in concrete can be obtained by measuring the resistance or current density.

Table 4
Estimation of corrosion probability as determined by half-cell potential test

Potential (mV), (CSE)	Probability of the presence of active corrosion
>−200	The probability for corrosion is very low
−200 to −350	Uncertain
<−350	The probability for corrosion is very high

Table 5
Microstructure and corrosion properties of the investigated steels

Specimen code	Microstructure	Volume fraction of pearlite/martensite	Corrosion current, I_{corr} (μA/cm^2)
FP	Ferrite–pearlite	0.14	0.15
IA25	Ferrite–chain martensite	0.24	0.18
IA50	Ferrite–chain martensite	0.31	0.26
IA75	Ferrite–chain martensite	0.38	0.29
IQ25	Uniform fibrous ferrite–martensite	0.37	0.28
IQ50	Uniform fibrous ferrite–martensite	0.41	0.34
IQ75	Uniform fibrous ferrite–martensite	0.49	0.41

Results of corrosion polarization studies of the developed materials with respect to a copper sulfate electrode are shown in Table 5. The data for corrosion current (I_{corr}) shown in Table 5 have been derived from the experimentally obtained cathodic polarization curves using Tafel's linear extrapolation method.

In the present contribution, the ferrite–pearlite structure shows highest corrosion resistance as compared to DP steels of any type. However, among the different DP steels the I_{corr} values are found to depend both on the relative amount and morphology of phase constituents. Although the martensite morphology remains almost similar as in IA25, IA50 and IA75 specimens or IQ25, IQ50 and IQ75 specimens, corrosion current (rate) value is found to increase with the amount of martensite.

As known, when the steel specimen either with ferrite–pearlite or ferrite–martensite structure corrodes in concrete, both the following reactions occur on the steel surface with ferrite acting as anode

$$Fe \rightarrow Fe^{2+} + 2e^{-}(\text{Anodic})$$

$$H_2O + 1/2O_2 + 2e^{-} \rightarrow 2(OH)^{-}(\text{Cathodic}).$$

It is observed from Table 5 that consequent to the increase in the amount of martensite brought about by using higher duration for austenization treatment in any heat treatment route, the amount of ferrite decreases. Such relative change in the amount of the phase constituents would lead to a change in the ratio of cathode to anode areas. Therefore, unfavorable area ratio between cathode (ferrite) and anode (martensite) brought about by increasing the amount of martensite justifies the observed higher corrosion rate of IA75 and IQ75 as measured in terms of I_{corr} compared to (IA25, IA50) and (IQ25, IQ50) specimens, respectively. The results of this study shows increased corrosion rate IQ25, IQ50 and IQ75 specimens compared to IA25, IA50 and IA75 specimens, respectively. This arises due to the variation in the morphology and distribution of the phase constituents. Since IQ treatment produces a very fine fibrous structure, it can be qualitatively said that the interfacial area between ferrite (cathode) and martensite (anode) is much more for IQ specimens compared to the specimens developed following IA route (IA25, IA50, IA75) resulting in higher corrosion rate for IQ treated specimen.

4. Conclusions

In this study, dual-phase steels with different morphologies were obtained from SAE1010 structural carbon steel. Then, corrosion behavior of these steels embedded in concrete was investigated. As a result, it has been shown that DP steels have lower corrosion resistance than reinforcing steel embedded in concrete. Furthermore, IA specimens obtained from intercritical annealing heat treatment have illustrated better corrosion resistance than IQ specimens obtained from intermediate quenching heat treatment. Because, finely distributed phase mixtures consisting of fer-

rite and martensite in IQ specimens lead to more corrosion cells which accelerate the corrosion rate. IA75 specimen has the higher corrosion rate (0.29 $\mu A/cm^2$) than IA50 (0.26 $\mu A/cm^2$) and IA25 (0.18 $\mu A/cm^2$) specimens. IQ specimens have also shown the similar results. The corrosion rates have been measured as 0.41 $\mu A/cm^2$ for IQ75, 0.34 $\mu A/cm^2$ for IQ50 and 0.28 $\mu A/cm^2$ for IQ25, respectively. Results of the investigation conclude that corrosion rate in concrete of dual-phase steels with ferrite–martensite structure depend upon the volume fraction and morphology of the phase constituents. Increasing the amount of martensite bears an adverse effect on the corrosion behavior of dual-phase steel embedded in concrete. A direct comparison about the corrosion tendency between DP steel and ferrite–pearlite structure is not possible due to the presence of different amounts and morphologies of second phase.

References

[1] Hertlein BH. Assessing the role of steel corrosion in the deterioration of concrete in the national infrastructure: a review of the causes of corrosion and current diagnostic techniques, corrosion forms and control for infrastructure. San Diego, CA: Publication ASTM, Race St., PA; 1991. p. 1916.

[2] Swarup J, Trikha DN. Corrosion of reinforcement in concrete structure under various conditions. Transactions of the Metals Finishers' Association of India 1996;5(1):15.

[3] Broomfield JP. Strategic highway research programmer on corrosion of steel in concrete. Bull Electrochem 1995;11(4):169.

[4] Broomfield JP. Corrosion and residual life in concrete structures-an overview. Bull Electrochem 1995;11(3):121.

[5] Ellis WE, Riggs EH, Butler WB. Comparative results of utilization of fly ash, silica fume and GGBFS in reducing the chloride permeability of concrete, durability of concrete. In: Second international conference, vol. 1. Montreal, Canada, 1991.

[6] Rasheeduzzafar, Al-Saadoun SS, Al-Gahtani AS. Reinforcement corrosion-resisting characteristics of silica-fume blended cement concrete. ACI Mater J 1992;89(4):337.

[7] Massazza F, Oberti G, Durability of pozzolonic cements and Italian experience in mass concrete, durability of concrete. In: Second international conference, vol. 2. Montreal, Canada, 1991, p. 1259.

[8] Sagues A, Powers R, Zayed A. In: Page CL, Treadway TWJ, Bomforth PB, editor. Marine environment corrosion of epoxy-coated reinforcing steel, corrosion of reinforcement in concrete, 1990, p. 539.

[9] Rasheeduzzafar, Dakhil FH, Bader MA, Khan MM. Performance of corrosion resisting steels in chloride bearing concrete. ACI Mater J 1992;89(5):439.

[10] Repas PE. Dual-phase and cold-forming vanadium steels in the automobile industry. Berlin: Vanitec; 1978.

[11] Davies RG, Magee CL. In: Davenport T, editor. Structure and properties of dual-phase steels. New York: AIME; 1979.

[12] Nakagawa AH, Thomas G. Metallurgical transactions A. Phys Metall Mater Sci 1985;16A:831.

[13] Thomas G. In: Taylor KA, Thomson SW, Fletcher FB, editors. Physical metallurgy of direct quenched steels. TMS; 1993. p. 265.

[14] Jha BK, Avtar R, Sagar DV. Transactions of the Indian institute of metals 1996;49(3):133.

[15] Aksoy M, Esin A. Improving the mechanical properties of structural carbon steel by dual-phase heat treatment. J Mater Eng 1988;10(4):281–7.

[16] Park KS, Park KT, Lee DL, Lee CS. Effect of heat treatment path on the cold formability of drawn dual-phase steels. Mater Sci Eng A 2007;449–451:1135–8.

[17] Sarkar PP, Kumar P, Mana KM, Chakraborti PC. Microstructural influence on the electrochemical corrosion behaviour of dual-phase steels in 3.5% NaCl solution. Mater Lett 2005;59:2488–91.

[18] Zhang C, Cai D, Liao B, Zhao T, Fan Y. A study on the dual-phase treatment of weathering steel 09CuPCrNi. Mater Lett 2004;58:1524–9.

[19] Trejo D, Monteiro P, Thomas G, Wang X. Mechanical properties and corrosion susceptibility of dual-phase steel in concrete. Cement Concrete Res 1994;24(7):1245–54.

[20] ASTM E112-96. Standard test methods for determining average grain size. ASTM International, 2004.

[21] ACI 211.1. Standard practice for selecting proportions for normal, heavyweight and mass concrete. American Concrete Institute, 1991.

[22] ASTM C 876-91. Standard test method for half-cell potentials of uncoated reinforcing steel in concrete, vol. 4.02. Philadelphia, USA: Annual Book of ASTM Standards; 1991.